

## PHYSICS CONTRIBUTION

# DOSE AND VOLUME REDUCTION FOR NORMAL LUNG USING INTENSITY-MODULATED RADIOTHERAPY FOR ADVANCED-STAGE NON-SMALL-CELL LUNG CANCER

HASAN MURSHED, M.D.,\* H. HELEN LIU, PH.D.,\* ZHONGXING LIAO, M.D.,\*  
JERRY L. BARKER, M.D.,\* XIAOCHUN WANG, PH.D.,\* SUSAN L. TUCKER, PH.D.,<sup>†</sup>  
ANURAG CHANDRA, M.D.,\* THOMAS GUERRERO, M.D., PH.D.,\* CRAIG STEVENS, M.D., PH.D.,\*  
JOE Y. CHANGE, M.D., PH.D.,\* MELINDA JETER, M.D.,\* JAMES D. COX, M.D.,\*  
RITSUKO KOMAKI, M.D.,\* AND RADHE MOHAN, PH.D.\*

\*Division of Radiation Oncology and <sup>†</sup>Department of Biomathematics, University of Texas M. D. Anderson Cancer Center, Houston, TX

**Purpose:** To investigate dosimetric improvements with respect to tumor-dose conformity and normal tissue sparing using intensity-modulated radiotherapy (IMRT) compared with three-dimensional conformal radiotherapy (3D-CRT) for advanced-stage non-small-cell lung cancer (NSCLC).

**Methods and Materials:** Forty-one patients with Stage III-IV and recurrent NSCLC who previously underwent 3D-CRT were included. IMRT plans were designed to deliver 63 Gy to 95% of the planning target volume using nine equidistant coplanar 6-MV beams. Inverse planning was performed to minimize the volumes of normal lung, heart, esophagus, and spinal cord irradiated above their tolerance doses. Dose distributions and dosimetric indexes for the tumors and critical structures in both plans were computed and compared.

**Results:** Using IMRT, the median absolute reduction in the percentage of lung volume irradiated to >10 and >20 Gy was 7% and 10%, respectively. This corresponded to a decrease of >2 Gy in the total lung mean dose and of 10% in the risk of radiation pneumonitis. The volumes of the heart and esophagus irradiated to >40–50 Gy and normal thoracic tissue volume irradiated to >10–40 Gy were reduced using the IMRT plans. A marginal increase occurred in the spinal cord maximal dose and lung volume >5 Gy in the IMRT plans, which could be have resulted from the significant increase in monitor units and thus leakage dose in IMRT.

**Conclusion:** IMRT planning significantly improved target coverage and reduced the volume of normal lung irradiated above low doses. The spread of low doses to normal tissues can be controlled in IMRT with appropriately selected planning parameters. The dosimetric benefits of IMRT for advanced-stage non-small-cell lung cancer must be evaluated further in clinical trials. © 2004 Elsevier Inc.

## INTRODUCTION

Lung cancer remains the most common cancer in the world and is the leading cause of cancer death in the United States (1, 2). Treatment of lung cancer is still a major challenge for modern medicine, even with combinations of surgery, chemotherapy, and radiotherapy (RT). The presence of viable tumors in >80% of non-small-cell lung cancer (NSCLC) patients after administration of a conventional radiation dose of about 60 Gy significantly hampers tumor control (3). In the Radiation Therapy Oncology Group Study 73-01 (4), the overall intrathoracic failure rate was as great as 52% in patients who received 40 Gy and 33% in those who received 60 Gy. Furthermore, the 3-year overall survival rate was only 10% in those who had local failure compared with 22% in those who had local control. Later, Vijayaku-

mar *et al.* (5) reported a correlation between the radiation dose administered and local control of NSCLC in available published data, noting that the radiation dose may have to be as high as 80 Gy to achieve a local control rate of 90%.

However, lung tumors are surrounded by highly radio-sensitive and low-density lung tissue. The vicinity of critical structures, including the lungs, esophagus, heart, and spinal cord, prevents the delivery of effective radiation doses to lung tumors. For example, Graham *et al.* (6) reported that after RT for NSCLC, Grade 2 or greater symptomatic pneumonitis could occur in 42% of patients in whom the total lung volume that had been irradiated to >20 Gy ( $V_{20}$ ) exceeded 40%. In the past, three-dimensional conformal RT (3D-CRT) made it possible to reduce the toxicity of RT in critical structures while treating lung tumors with somewhat

Reprint requests to: H. Helen Liu, Ph.D., Division of Radiation Oncology, Unit 94, University of Texas M. D. Anderson Cancer Center, 1515 Holcombe Blvd., Houston, TX 77030. Tel: (713) 745-4502; Fax: (713) 745-4505; E-mail: hliu@mdanderson.org

Partially supported by Grant RO1 CA 74043 from the National Cancer Institute.

Received Jun 17, 2003, and in revised form Sep 5, 2003. Accepted for publication Sep 17, 2003.

escalated doses (7–9). The potential benefits of 3D-CRT can be greatly enhanced with the use of an emerging modality—intensity-modulated RT (IMRT). Currently, the promise of IMRT is being investigated for disease in various sites, including head-and-neck and prostate cancers (10).

In IMRT, intensity modulation within a radiation beam is designed on the basis of the target prescription and a set of dose constraints for sensitive structures using inverse planning algorithms. The capability of differentiating the weight of individual rays of a beam in IMRT allows sculpting of the isodose distributions to achieve dose conformity and avoidance. However, the role of IMRT in treating NSCLC remains largely unknown owing to the concern that IMRT may deliver a low, yet damaging, dose to normal lung tissue (11). In addition, lung tumor motion and the inhomogeneity of the region may cause a significant degree of dose deviation and uncertainty, and thus adverse effects on tumors and normal tissues.

In a preliminary study, we investigated the feasibility of using IMRT for Stage I-III B NSCLC and whether low-dose exposure to lung tissue can be controlled and minimized with IMRT (12). The results suggested that with an appropriate radiation beam configuration and IMRT optimization criteria, it is possible to reduce the lung volume exposed to damaging doses. In a continuation of this earlier work, the goal of the current research was to focus on a larger patient population with advanced-stage disease and to assess the potential dosimetric benefits of IMRT further. In particular, we intended to select a group of patients who represent the most typical patient population undergoing RT for NSCLC and who remain a challenge for conventional 3D-CRT. This comprehensive dosimetric study was designed in preparation for the clinical implementation of IMRT for NSCLC and upcoming clinical trials of treating NSCLC using dose escalation.

## METHODS AND MATERIALS

### Patient selection

We expanded our preliminary preclinical dosimetric study (12) to include a much larger and more homogenous patient population. A total of 41 patients, most having Stage III NSCLC recently treated with chemoradiation, were selected for this study. The histologic subtypes included NSCLC (adenocarcinoma and squamous cell carcinoma) and other types of thoracic cancer. The NSCLC patients included a homogenous group with locally advanced unresectable Stage IIIA, IIIB, or IV disease and a few with recurrent disease. The location of each tumor was defined as the right or left lung depending on the location of the primary disease and superior or inferior depending on whether >50% of the planning target volume (PTV) was located superior or inferior to a line bisecting the individual lungs. The patient characteristics are summarized in Table 1. Most patients received concurrent carboplatin- and paclitaxel-based chemotherapy. A few patients received neoadjuvant chemotherapy or no chemotherapy according to the

Table 1. Patient characteristics

	<i>n</i>	
Age (y)		
Median	66	
Range	23–80	
Gender		
Male	25	(60)
Female	16	(40)
Histologic subtype		
Adenocarcinoma	14	(34)
Squamouscarcinoma	16	(39)
NSCLC, NOS	9	(22)
Other	2	(5)
Stage		
IIIA	16	(39)
IIIB	17	(41)
IV	2	(5)
Recurrent	6	(15)
Location		
Right	21	(51)
Left	20	(49)
Upper	32	(78)
Lower	9	(22)
GTV (cm <sup>3</sup> )		
Median	121	
Range	4–535	
PTV (cm <sup>3</sup> )		
Median	623	
Range	75–1645	

*Abbreviations:* NSCLC = non-small cell lung cancer; NOS = not otherwise specified; GTV = gross tumor volume; PTV = planning target volume.

Data presented as number of patients, with percentage in parentheses, unless otherwise specified.

preference of the referring medical oncologists. We intended to select those cases with relatively large tumors (as is the nature of advanced-stage NSCLC) located in the upper lobe of the lung, and/or attached to the mediastinum or chest wall. Thus, the respiratory-induced tumor motion could be less compared with Stage I-II cases, a finding drawn from a separate in-house tumor motion study and a published study (13).

### 3D-CRT technique

All the patients in this study had previously undergone 3D-CRT. CT simulation was performed with images at 3-mm slice intervals over the entire thorax. The patients were placed in the supine position with their arms above their head in an immobilization device. CT scans were obtained during normal respiration with no special breathing instructions. The target volume and all critical structures were then drawn on the scans. The gross tumor volume (GTV) was defined as the visualization of any gross disease and lymph nodes  $\geq 1$  cm on CT. The clinical target volume was defined as the GTV plus a 6- to 8-mm margin (adenocarcinoma, 8 mm; squamous cell carcinoma, 6 mm). The PTV was defined as the clinical target volume plus an 8–12-mm margin to account for tumor motion and setup

uncertainty. To account for the beam penumbras, a 5-mm margin from the PTV to the block edge was then added. In addition, the critical structures, including both lungs and the heart, esophagus, and spinal cord, were contoured. The total normal lung excluded the GTV, however. Beam's eye view displays were used to select three to six AP and oblique beams with a combination of 6-MV and 18-MV photon beams. The dose calculation was based on the convolution/superposition algorithm, including a full heterogeneity correction using a commercial treatment-planning system (Pinnacle<sup>3</sup>, Philips Medical Systems, Andover, MA). The radiation dose was 180 cGy given each day for a total of 63 Gy in 35 fractions prescribed to 95% of the PTV in all cases. The dose delivered to the normal lung was minimized in designing the 3D-CRT plans so that the lung  $V_{20}$  was <40%, if possible. The maximal dose delivered to the spinal cord was kept <45 Gy.

#### IMRT technique

The actual 3D treatment plans were retrieved and re-planned for the IMRT study using the same treatment planning system. This system uses a gradient-search based inverse planning algorithm to generate optimal beam fluences, for which planners specify the dose objectives/constraints for the target and all other normal structures. The goal of optimization in the present study was to minimize an objective function as defined on the basis of the difference between the desired and calculated doses for the target and all specified critical organs.

In the IMRT plans, nine equidistant, coplanar, axial 6-MV beams were used. The target volumes, isocenter, and prescription were kept the same as those in the 3D treatment planning. Additional planning structures were delineated to achieve satisfactory IMRT plans. These structures included the planning spinal cord and planning esophagus, with a 0.5-cm margin expansion of the original structures. The planning normal tissue included all the tissues enclosed by the skin, except for a structure that was expanded from the PTV with a 1-cm margin. The planning objectives for the IMRT plans reflected the following priorities: (1) achieving tumor dose coverage at the prescription dose; (2) keeping the maximal dose of the planning spinal cord  $\leq 45$  Gy; (3) reducing the  $V_{20}$  and volume of the normal lung receiving  $\geq 5$  ( $V_5$ ) and  $\geq 10$  Gy ( $V_{10}$ ); (4) reducing the volume of the planning esophagus and heart receiving 45 ( $V_{45}$ ) and 50 Gy ( $V_{50}$ ); and (5) reducing the  $V_{50}$  of the planning normal tissues in the thorax. Multiple iterative processes were required until the objective function was minimized and the treatment planning goals were met.

After inverse planning, the leaf motion required for the accelerator (Varian 2100EX with a 120-leaf Millennium multileaf collimator (MLC), Varian Oncology Systems, Palo Alto, CA) using the sliding window technique (14) was generated for all of the IMRT plans. This was achieved using an in-house leaf conversion software program that has been tested for clinical implementation at our institution. The actual beam fluence delivered by the leaf motion was

then used to compute the deliverable dose distribution method with tissue heterogeneity correction. The accuracy of the dose calculation for the IMRT plans was verified by measurement.

#### Treatment plan evaluation

Dosimetric comparison of the 3D-CRT and IMRT plans was carried out for each patient. Isodose distributions, dose-volume histograms (DVHs), and various dosimetric parameters were generated and calculated for both plans. To evaluate the quality of the plans in treating the tumors, the conformity index (CI) and heterogeneity index (HI) were computed on the basis of the DVHs of the PTVs. The CI was defined using the equation

$$CI = V_{dp}/V_{ptv}, \quad (1)$$

where  $V_{dp}$  is the volume enclosed by the 63-Gy prescription isodose surface and  $V_{ptv}$  is the volume of the PTV. A larger CI indicated a greater volume of the prescription dose delivered outside the PTV. The HI was defined using the equation

$$HI = D5\%/D95\%, \quad (2)$$

where D5% and D95% correspond to the dose given to 5% and 95% of the PTV, respectively. A larger HI indicated a greater dose exceeding the prescription dose, and thus, greater dose heterogeneity inside the PTV.

The  $V_5$ ,  $V_{10}$ ,  $V_{20}$ , mean dose, and integral dose for the total lung were calculated for the comparisons. The integral dose was defined using the equation

$$ID = \sum_i D_i^* V_i^* \rho_i, \quad (3)$$

where  $V_i$  is the volume of the lung irradiated at a dose of  $D_i$  and  $\rho_i$  is the local density of  $V_i$ . The integral dose describes the total energy imparted to certain structures, in this case, the entire lung tissue, excluding the GTV.

Because of the observed differences in the physical dose delivered to the lung between 3D-CRT and IMRT planning, the normal tissue complication probability (NTCP) of radiation pneumonitis was calculated using the Kutcher-Burman histogram reduction scheme (15) in conjunction with the Lyman model (16). This model uses three parameters, including the dose that would cause 50% complication probability ( $TD_{50}$ ), a volume dependence exponent of the complication probability ( $n$ ), and a steepness parameter for the dose complication curve ( $m$ ). Investigators have reported several sets of values for these parameters in the literature. Thus, we decided to test two different sets of parameters for comparison of 3D-CRT and IMRT in this study. The first set was the well-established parameters described by Burman *et al.* (17) in which  $TD_{50} = 24.5$  Gy,  $n = 0.87$ , and  $m = 0.18$  according to the clinical review by Emami *et al.* (18). The second set was the clinical param-

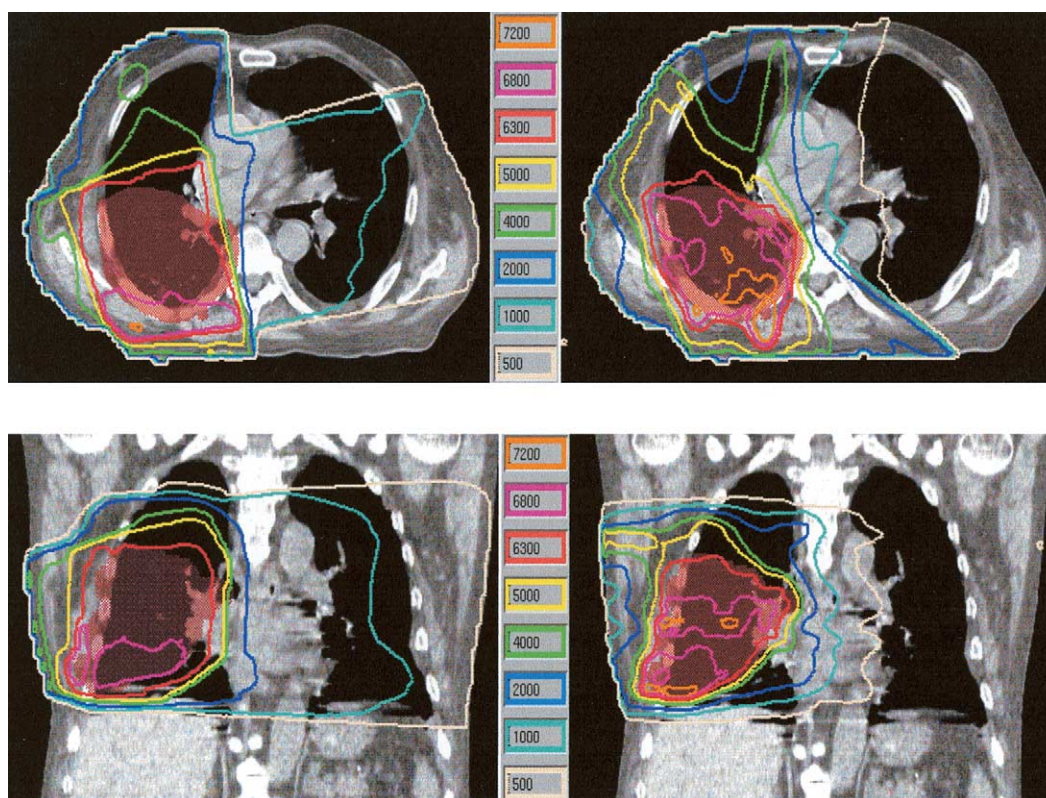


Fig. 1. Comparison of isodose distribution with (Left) 3D-CRT and (Right) IMRT in a single case. (a) Axial view. (b) Coronal view.

eters described by Hayman *et al.* (19) in which  $TD_{50} = 33$  Gy,  $n = 1.00$ , and  $m = 0.33$ , as determined by the data collected from their Phase I dose-escalation NSCLC trial. Using these parameters, the NTCP of radiation pneumonitis was calculated for the total lung for each patient's 3D-CRT and IMRT plan.

In addition to the NTCP models described above, in comparing the risk of radiation pneumonitis, we also modeled the NTCP using the results presented by Graham *et al.* (20) with the lung  $V_{20}$  as the predictive variable and those presented by Yorke *et al.* (21) and Kwa *et al.* (22), with the total lung mean dose (TLMD) as the predictive variable. In general, these models assumed that the risk of pneumonitis increased with the dosimetric variables (either  $V_{20}$  or TLMD). Thus, the risk of pneumonitis was interpolated on the basis of the data presented in these studies.

For the other critical thoracic structures, the volume of the esophagus irradiated to  $>55$  Gy, heart to  $>40$  Gy, and spinal cord to  $>45$  Gy, 50 Gy, and its maximal dose were also calculated in the dosimetry comparison of the 3D-CRT and IMRT plans.

The integral dose delivered to the entire thorax and the  $V_5$ ,  $V_{10}$ ,  $V_{20}$ ,  $V_{30}$ , and  $V_{40}$  of the thorax were calculated as well. The total thorax included all the tissue enclosed by the skin surface. The purpose was to investigate the possible increase in the integral dose delivered to the normal thoracic tissue and total volume of normal tissue exposed to the low doses in IMRT compared with 3D-CRT planning. In addition,

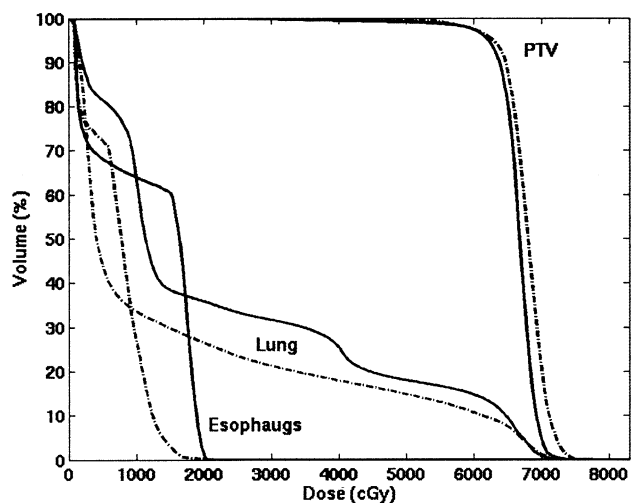
the total number of monitor units (MUs) for 3D-CRT and IMRT was also investigated.

The various dosimetric and NTCP parameters for 3D-CRT and IMRT planning as noted above were the primary end points for this study and were analyzed using descriptive statistics. The statistical significance of comparing these parameters was determined using the Wilcoxon signed rank test. Differences were reported to be statistically significant at  $p \leq 0.05$ . Statistical analysis was performed using the StatView for Windows software program (version 5.0.1, SAS Institute, Cary, NC).

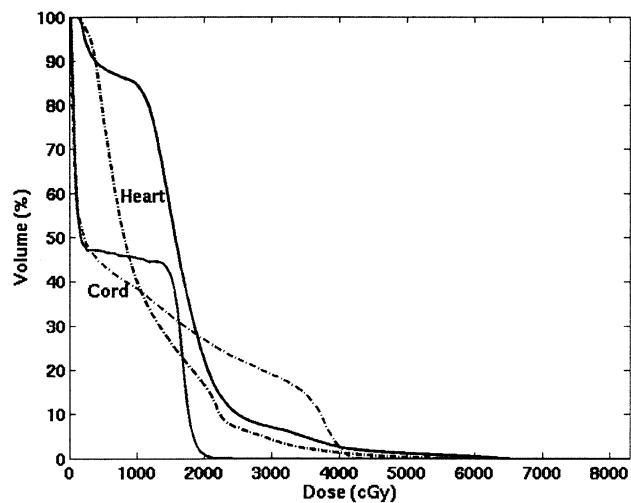
## RESULTS

### Isodose and DVHs

Typical 3D-CRT and IMRT plans for one of the study patients are presented in Fig. 1. This patient had a very large PTV of  $1108 \text{ cm}^3$  occupying a significant portion of the right lung. The IMRT isodose distribution showed that the 63 Gy prescription isodose line was highly conformal to the PTV in all three planes, with a CI of 1.14 compared with 1.42 in the 3D-CRT plan, an improvement of 28%. Also, the isodose lines of 40 and 50 Gy were pushed away from the spinal cord in the IMRT plans, with the low isodose lines of 5–20 Gy sparing more lung tissue in both the ipsilateral and the contralateral lung. Although nine equidistant beams were used to irradiate the tumor from different angles, the IMRT optimization algorithm was able to minimize the



(a)



(b)

Fig. 2. Comparison of dose-volume histograms (DVHs) with three-dimensional conformal radiotherapy (3D-CRT) (solid lines) and intensity-modulated radiotherapy (IMRT) (dashed lines) in the same case as that in Fig. 1. (A) DVHs of planning tumor volume (PTV), total lung, and esophagus. (B) DVHs of spinal cord and heart.

beams on the left side of the patient to spare the contralateral lung and deliver the radiation dose from the right anterior and left posterior directions while sparing the spinal cord.

A comparison of the DVHs for 3D-CRT and IMRT in the same patient is shown in Fig. 2. The maximal tumor dose increased slightly with IMRT compared with 3D-CRT, with an HI of 1.11 and 1.14, respectively, a detriment of 3% for IMRT. The DVHs for the total lung showed an approximately 40% reduction in the  $V_5$ , a 30% reduction in the  $V_{10}$ , and a 10% reduction in the  $V_{20}$  using the IMRT plan. The esophageal DVHs for both the IMRT and the 3D-CRT plans did not show a significant volume  $>55$  Gy. The DVHs for the heart with IMRT and 3D-CRT were similar, showing no increase in the heart dose with 3D-CRT compared with that with IMRT. Finally, the spinal cord DVHs did not show a significant  $V_{45}$  and  $V_{50}$  in the IMRT plan, although with IMRT, the maximal cord dose increased to 43.2 Gy but still remained less than the 45-Gy constraint.

#### Target conformity

The IMRT plans, in general, were more conformal, with a CI improved as high as 70% in individual cases and an average improvement of 21% for all cases. The median CI in the IMRT plans was 1.41, a statistically significant improvement compared with the median CI of 1.54 in the 3D-CRT plans ( $p = 0.004$ ; Table 2).

#### Target heterogeneity

The IMRT plans, in general, increased the target heterogeneity to a small degree. The median target HI was 1.16 in the IMRT plans compared with 1.12 in the 3D-CRT plans ( $p = 0.0004$ ; Table 2). The minimal PTV dose was 55.1 Gy in the IMRT plans vs. 55.8 Gy in the 3D plans. Although a decrease resulted in this dose, the reduction was not significant either clinically or statistically. For certain cases, the minimal PTV dose was affected by the proximity of the spinal cord, which had a greater priority of receiving  $<50$  Gy than treating the PTV. The GTV and clinical target volume received approximately the full prescription dose in both sets of plans, which was our standard clinical practice.

#### Lung $V_5$ , $V_{10}$ , and $V_{20}$

The median  $V_5$  of the lung did not significantly increase using IMRT ( $p = 0.4239$ ). In approximately 63% of the cases, however, the lung  $V_5$  increased for the reasons described below. The median  $V_{10}$  and  $V_{20}$  of the lung was 38% and 25%, respectively, using the IMRT plans, a reduction of 7% and 10%, respectively, from that using the

Table 2. Summary of CI, HI, and number of MUs for 3D-CRT and IMRT plans

Parameter	3D-CRT	IMRT	$p$
CI	1.54 (1.26–4.53)	1.41 (1.06–2.09)	0.004
HI	1.12 (1.06–1.22)	1.16 (1.06–1.43)	0.004
Minimal PTV dose (Gy)	56.5 (38.4–62.0)	55.8 (44.4–64.0)	0.060
MUs (sliding window)	266 (166–991)	1884 (953–3838)	$<0.0001$

Abbreviations: CI = conformity index; HI = heterogeneity index; MUs = monitor units; 3D-CRT = three-dimensional conformal radiotherapy; IMRT = intensity-modulated radiotherapy.

Data presented as the median, with the range in parentheses.

Table 3. Summary of the total lung  $V_5$ ,  $V_{10}$ , and  $V_{20}$ ,  $V_{\text{eff}}$ , mean dose, and integral dose for 3D-CRT and IMRT plans

Parameter	3D-CRT	IMRT	<i>p</i>
Total lung $V_5$ (%)	52 (28–86)	59 (25–78)	0.424
Total lung $V_{10}$ (%)	45 (22–64)	38 (18–59)	<0.0001
Total lung $V_{20}$ (%)	35 (17–55)	25 (13–43)	<0.0001
Total lung $V_{\text{eff}}$ (%)	71 (33–101)	58 (28–95)	<0.0001
Total lung mean dose (Gy)	19 (10–29)	17 (9–27)	<0.0001
Total lung integral dose (J)	19 (5–36)	16 (5–34)	<0.0001

Abbreviations:  $V_5$ ,  $V_{10}$ ,  $V_{20}$  = volume irradiated to >5, >10, >20 Gy;  $V_{\text{eff}}$  = effective volume; other abbreviations as in Table 2.

Data presented as the median, with the range in parentheses.

3D-CRT plans ( $p \leq 0.0001$ ; Table 3). Figure 3 summarizes the distribution of the  $V_5$ ,  $V_{10}$ , and  $V_{20}$  in the 3D-CRT and IMRT plans. The results also showed the general trend of the DVHs in comparing the 3D-CRT and IMRT plans, specifically, that the  $V_{10}$ ,  $V_{20}$  were significantly reduced with the IMRT plans.

Mean total lung and integral dose

The TLMD decreased from 19.21 Gy with 3D-CRT to 17.20 Gy with IMRT, a statistically significant difference ( $p < 0.0001$ ). The same trend was observed for the integral dose delivered to the lung (i.e., the median reduction in the lung integral dose was 2.8 J in the IMRT plans; Table 3).

Radiation pneumonitis risk

The Lyman NTCP model indicated that the risk of radiation pneumonitis can be reduced with the IMRT plans compared with the 3D-CRT plans. Using the parameters described by Burman *et al.* (17), we estimated that the median pneumonitis risk would decrease from 36% with the 3D-CRT plans to 9% with the IMRT plans. However, using the parameters described by Hayman *et al.* (19), it was estimated that the median pneumonitis risk would decrease from 13% with the 3D-CRT plans to 7% with the IMRT plans. The reduction in the risk of pneumonitis was statistically significant using both sets of parameters (Table 4). The results obtained using the models presented by Graham

Table 4. Summary of risk of radiation pneumonitis as estimated from  $V_{20}$ , TLMD, and NTCP models

Parameter	3D-CRT	IMRT	<i>p</i>
RPR from $V_{20}$ (20)	20 (2–65)	6 (1–37)	NA
RPR from MLD (21)	22 (4–7)	16 (4–62)	NA
RPR from MLD (22)	12 (1–45)	9 (1–38)	NA
RPR from NTCP (17)	36 (0–90)	9 (0–82)	<0.0001
RPR from NTCP (19)	13 (2–34)	7 (1–27)	<0.0001

Abbreviations:  $V_{20}$  = volume irradiated to >20 Gy; TLMD = total lung mean dose; NTCP = normal tissue complication probability; RPR = radiation pneumonitis risk; MLD = mean lung dose; other abbreviations as in Table 2.

Data presented as the median, with the range in parentheses.

*et al.* (20) with the lung  $V_{20}$  as the predictive variable and by Yorke *et al.* (21) and Kwa *et al.* (22) using the total lung mean dose as the predictive variable are included in Table 4 as well. The percentage in the reduction in the risk of pneumonitis ranged from 3% using the Kwa data to 27% using the Burman data.

Improvement in  $V_{20}$  and TLMD with IMRT as a function of tumor size and location

Regression analysis showed no statistically significant correlation between IMRT and 3D-CRT  $V_{20}$  differences and tumor size (neither the GTV nor PTV). However, as the PTV increased, sparing of the lung with IMRT at the  $V_{20}$  decreased slightly, with an  $r^2$  value of 0.051. However, this correlation was not statistically significant ( $p = 0.1722$ ). A similar finding was noted for the total lung mean dose: as the PTV increased, the difference in the mean total lung dose between IMRT and 3D-CRT decreased slightly, with an  $r^2$  value of 0.034. This correlation also was not statistically significant ( $p = 0.2671$ ). The improvement in lung sparing at the  $V_{20}$  and total lung mean dose with IMRT was also analyzed as a function of tumor location (right or left, upper or lower). None of the parameters were found to have a significant effect on the degree of lung sparing.

Esophagus, heart, and spinal cord

The dose delivered to the esophagus and heart was not increased in the IMRT plans; in most cases, it was reduced. Table 5 shows that the median  $V_{55}$  of the esophagus with IMRT was 7% lower than that with 3D-CRT. A reduction in the median  $V_{40}$  of the heart was also observed, although the degree of the reduction was less than that in the esophagus. The median  $V_{45}$  of the spinal cord (the true spinal cord without margin expansion) was <1% with IMRT. In addition, the median maximal spinal cord dose was 45.8 Gy with 3D-CRT and 48.6 Gy with IMRT, an increase that was acceptable for clinical treatment. For a few cases, a very small fraction of the spinal cord was allowed to exceed 50 Gy if GTV was present near the spinal cord.

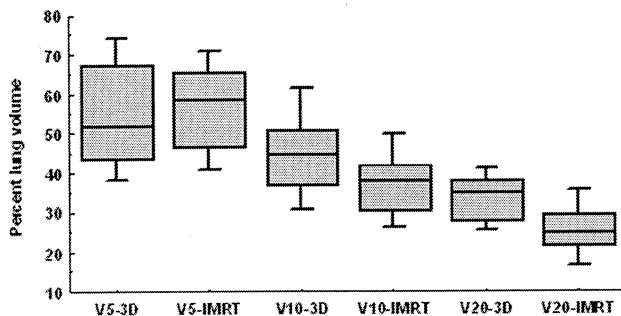


Fig. 3. Summary of total lung  $V_5$ ,  $V_{10}$ , and  $V_{20}$  with three-dimensional conformal radiotherapy (3D-CRT) and intensity-modulated radiotherapy (IMRT) plans.

Table 5. Summary of the esophagus, heart, and spinal cord volumes irradiated

Parameters	3D-CRT	IMRT	<i>p</i>
Esophagus (% volume at 55 Gy)	35.0 (0.0–72.0)	28.8 (0.0–71.0)	<0.0001
Heart (% volume at 40 Gy)	13.0 (0.0–58.0)	11.0 (0.0–59.0)	0.004
Spinal cord (% volume at 45 Gy)	0.0 (0.0–33.0)	0.9 (0.0–31.0)	0.026
Spinal cord (% volume at 50 Gy)	0.0 (0.0–4.3)	0.0 (0.0–9.0)	0.523
Spinal cord (maximal dose, Gy)	45.8 (10.6–55.4)	48.6 (38.6–63.2)	0.0002

Abbreviations as in Table 2.

Data presented as the median, with the range in parentheses.

#### Normal thoracic tissue $V_5$ , $V_{10}$ , $V_{20}$ , $V_{30}$ , $V_{40}$ , and integral dose

Table 6 shows that with IMRT planning, the median integral dose delivered to the thorax was increased slightly (5 J) compared with 3D-CRT planning, although this difference was not statistically significant ( $p = 0.7805$ ). A close observation of the integral dose in the two planning types showed that it was fairly comparable. However, the median  $V_5$  of the normal thoracic tissue was 1270 cm<sup>3</sup> greater in the IMRT plans than in the 3D-CRT plans ( $p = 0.006$ ). The  $V_{10}$  of the normal thoracic tissue in the two plans was found to be comparable, although the volume increased in one-half of the cases with IMRT. In contrast, the  $V_{20}$ ,  $V_{30}$ , and  $V_{40}$  of the normal tissue all significantly decreased with IMRT planning owing to the increased dose conformity to the target volume (Table 6).

#### Total MUs

On average, the 3D-CRT plans required 266 MUs to deliver one fraction of the treatment. The IMRT plans required approximately 1000 MUs before and 1884 MUs after MLC leaf conversion using the sliding window technique (Table 2). The large MUs used in the IMRT plans were primarily caused by the use of the sliding window technique for the leaf-sequence conversion. We found that use of a step-and-shoot leaf sequence with a more efficient delivery algorithm could reduce the sliding-window MUs by one-half.

## DISCUSSION

In this study, we investigated the effect of IMRT for NSCLC through a retrospective dosimetric analysis. In to-

tal, 41 lung cancer cases were used in the comprehensive analysis for IMRT planning, of which 33 were Stage IIIA or IIIB NSCLC. The reasons for choosing mainly cases of Stage III disease for this study were twofold. First, this group of patients represents the typical NSCLC patient population seen in our radiation oncology clinic. The disease is often a challenge when using conventional 3D treatment planning because of the extent of tumor growth and lymph node involvement. Second, in our earlier work, in which the feasibility of IMRT was established for NSCLC (12), we found that IMRT may be more suitable than 3D treatment planning for cases of advanced-stage disease with a relatively larger GTV and thus a greater volume of normal lung involvement. Therefore, the main focus of the present research was to identify the potential benefits of IMRT for this group of patients, in whom local tumor control and a reduction in treatment toxicity have been traditionally very difficult to achieve.

Even in this relatively homogenous patient population, the spectrum of tumor sizes was still wide (Table 1), representing different disease anatomies and morphologies. Nevertheless, we saw a significant improvement in the conformity of the prescription dose in all cases. Both the median value and the range of the CI decreased with IMRT (Table 2 and Fig. 3), indicating a greater ability to warp high-dose volumes around tumors by introducing intensity modulation within the beams. Although the dose heterogeneity was slightly elevated in the IMRT plans, the increase in the dose heterogeneity within the tumor was considered clinically acceptable and may even be beneficial in treating aggressive disease. For example, in treating head-and-neck cancer, a high dose delivered inside the target has intentionally been used to design a new accelerated fractionation

Table 6. Summary of the normal thoracic tissue  $V_5$ ,  $V_{10}$ ,  $V_{20}$ ,  $V_{30}$ , and  $V_{40}$  and integral dose

Parameter	3D-CRT	IMRT	<i>p</i>
Thoracic normal tissue $V_5$ (cm <sup>3</sup> )	5658 (3040–11596)	6929 (2759–10788)	0.006
Thoracic Normal Tissue $V_{10}$ (cm <sup>3</sup> )	4905 (2550–8751)	4931 (2066–8722)	0.636
Thoracic Normal Tissue $V_{20}$ (cm <sup>3</sup> )	3919 (1919–6776)	3398 (1509–6535)	0.001
Thoracic Normal Tissue $V_{30}$ (cm <sup>3</sup> )	3212 (1560–5489)	2673 (1242–5402)	<0.0001
Thoracic normal tissue $V_{40}$ (cm <sup>3</sup> )	3213 (1560–5489)	2673 (1242–5402)	<0.0001
Thoracic normal tissue integral dose (J)	180 (88–311)	185 (72–13511)	0.781

Abbreviations as in Tables 2 and 3.

Data presented as the median, with the range in parentheses.

scheme of simultaneous integrated boost (23). The simultaneous integrated boost technique simultaneously delivers doses at different levels to different targets in a single treatment session and may be used for dose escalation in NSCLC patients.

Similar to our findings in this work, the dosimetric benefits of IMRT have been studied more extensively and are well established for other tumor sites. Eisbruch *et al.* (24) and Xia *et al.* (25) showed improved tumor coverage and sparing of the parotid glands with IMRT for head-and-neck cancers. More recently, Zelefsky *et al.* (26) reported that prostate cancer patients who underwent IMRT had decreased acute and late rectal toxicity compared with those who underwent 3D-CRT. Although the promise of IMRT has been demonstrated in the sites listed above, the role of IMRT has not been widely investigated and accepted for lung cancer. The major obstacles arise from the fact that lung tissue is highly radiosensitive and exhibits a greater degree of volume dependence than do other tissues. Thus, there is a general concern and assumption that IMRT may not be applicable for NSCLC because of the risk of delivering low, yet damaging, doses to a larger volume of lung tissue surrounding the tumor. In addition, the possible movement of a tumor owing to respiration introduces another level of complexity to both the IMRT dosimetry and technique used.

Therefore, the first priority of our research was to address the question of whether IMRT can be used to reduce the lung volume treated above low doses (such as 10 and 20 Gy). On the basis of previous studies of the lung toxicity from RT (17–22), we have used a variety of dosimetric and radiobiologic indexes, including the  $V_5$ ,  $V_{10}$ ,  $V_{20}$ , and mean and integral dose, as well as NTCP models, in comparing the isodose distributions of the IMRT and 3D-CRT plans. The results given in Tables 3 and 4 and Fig. 3 show the advantage of using IMRT to reduce the lung  $V_{10}$  and  $V_{20}$ , with a median reduction of 7% and 10%, respectively. However, the benefit of IMRT was diminished at lower doses, although the  $V_5$  was still reduced with IMRT in about one-half of the cases. When the mean and integral doses delivered to the lung were used for the comparison, we saw a median reduction of 2 Gy and 2.8 J, respectively, for normal lung tissue (Table 4).

A great degree of uncertainty is associated with assessment of the lung toxicity of RT. Graham *et al.* (20) reported that the risk of radiation pneumonitis correlated with the  $V_{20}$  of the lung. In contrast, Yorke *et al.* (21) and Kwa *et al.* (22) found that the mean lung dose was a better indicator of this risk using a greater, yet mixed, patient population from a variety of disease sites. In addition, there is also a discrepancy in the  $TD_{50}$  values reported in different studies, although, in general, the tolerance dose delivered to the lung is believed to range from 20 to 30 Gy (17–22).

To comprehend the effect of lung irradiation using IMRT, we must resort to the use of two distinct sets of NTCP parameters to estimate the risk of radiation pneumonitis. The Lyman model assumes that the probability of pneumonitis after homogenous irradiation follows a sigmoidal dose–response relationship (16). Kutcher and Burman

(15) developed a DVH reduction scheme for heterogenous irradiation in which the DVH is converted to an effective volume using a power-law relationship. The first application of such a model by Burman *et al.* (17) in 1991 resulted in the estimated parameters of  $TD_{50} = 24.5$  Gy,  $n = 0.87$ , and  $m = 0.8$ . However, in 2001, Hayman *et al.* (19) reported that after correcting for lung inhomogeneity, the modified parameters were  $TD_{50} = 33$  Gy,  $n = 1.0$ , and  $m = 0.33$ , on the basis of their Phase I NSCLC dose-escalation trial. Apparently, the first set of parameters predicted a greater median pneumonitis risk (36% for 3D-CRT) compared with the second set of parameters (13% for 3D-CRT). We believe that the estimated NTCP using the parameters from the study by Hayman *et al.* is much closer to that in our clinical reality; thus, it may be more applicable for this study. The estimated risk of pneumonitis has a large disparity from existing studies, indicating a large degree of uncertainty in the NTCP models. The reduction in the risk of pneumonitis ranged from 3% with the model by Kwa *et al.* (22), 6% using the model of Hayman *et al.* (19) and Yorke *et al.* (21), to 12% using the model by Graham *et al.* (20).

Although the reduction in the  $V_{20}$ , mean lung dose, and NTCP models all predicted a positive effect of IMRT on lung sparing, we should keep in mind that the predictions were based on experience with conventional RT. Currently, no biologic or clinical data are available to support the NTCP model for IMRT, especially with more aggressive, concurrent chemoradiation. In addition, we could not reduce the lung  $V_5$  in more than 50% of cases, even using IMRT. The increase in the  $V_5$  with IMRT was possibly caused by transmission and leakage of the MLCs, as evident by the approximately sevenfold increase in the number of MUs required for delivery of IMRT. Accordingly, the  $V_5$  for the total thoracic tissue also increased for the same reason. Because of a lack of radiobiologic data for such low-dose RT (<14 cGy/fraction), it is unknown whether such an increase in the low-dose volume of the lung and unspecified normal tissue will cause serious side effects and modification of the toxicity profile. Thus, the clinical feasibility of using IMRT for lung cancer and whether lung toxicity can indeed be demonstrably reduced must be assessed rigorously in future clinical studies.

We believe that the most significant finding in the present study was that IMRT can be used to reduce the  $V_{10}$  and  $V_{20}$  for normal lung tissue and that the spread of low doses can be controlled in a predictive manner with IMRT, even with a large number of beams. We intentionally chose to use nine coplanar beams in the IMRT plans in all the cases to test our hypothesis. From a physics perspective, such a reduction of the low-dose volume is possible with IMRT because of the additional degree of freedom introduced by the variable intensities within the beams. Such an arrangement allows for sculpting and fine tuning of the isodose distributions. In other words, if the constraints for low-dose volumes are properly included in the inverse planning process, it is highly likely that the resulting dose distributions will reflect such considerations of the planners. To some extent, an increased low-dose volume is not the definite consequence of IMRT but rather the consequence of

exclusion of such considerations from treatment planning. However, owing to physical limitations, such as transmission and leakage of MLCs, a reduction of low-dose volumes, such as that  $>5$  Gy, may not be significant or completely possible, even though such constraints were included. In our earlier work, we found that by using fewer beams or segments, IMRT could lead to an additional reduction of the  $V_5$  for lung and thoracic tissue. Thus, when using IMRT for lung cancers, it is imperative to minimize the leakage dose and improve the MU efficiency in the delivery of the beams. Developing more efficient IMRT delivery with optimization and reduction of the beam angles will be studied further in our future research.

In addition to the possibility of sparing the lung, we observed that the esophagus and heart volumes  $>45$ – $55$  Gy did not increase with the use of IMRT. In most cases, these volumes were reduced with IMRT compared with 3D-CRT. Because acute esophagitis and long-term cardiac toxicity can be significant limiting factors in the treatment of lung cancer, dose reduction for these structures should benefit this treatment as well.

As far as the entire thoracic tissue is concerned, the  $V_{20}$  and greater dose volumes were all reduced with IMRT, apparently because of the increased high-dose conformity. As a result, the integral dose delivered to the patient was also reduced with IMRT in certain cases, contradictory to the commonly held belief that IMRT will increase the integral dose delivered to normal tissue. However, the  $V_5$  of the thorax increased, possibly because of the MLC leakage with the increased MUs of the IMRT as discussed above. The biologic effect of the tradeoff between a reduction of the high dose and an increase in the low dose for IMRT is still unknown. Apparently, a more efficient delivery system for IMRT is highly desirable to reduce the total number of MUs and consequently the low dose delivered to the patients and staff. We found that the use of a step-and-shoot leaf sequence could potentially reduce the MUs by one-half compared with the sliding window technique, which may help to reduce the lung and normal tissue volumes at very low doses.

With respect to the complexity of the treatment planning in the present study, it did take considerably more time to optimize and finalize the IMRT plans compared with the 3D-CRT plans. However, as we become more familiar with the behavior of the inverse planning system and the choice of optimization parameters, we expect to reduce the total IMRT planning time. Even so, further improvement of the efficiency and throughput of IMRT plans is urgently needed. This may be accomplished by prescreening the NSCLC cases that will benefit most from IMRT. In the patients in our study, because no statistically significant correlation was found between the extent of lung

sparing and tumor size or location, we believe that IMRT may be suitable for treating all cases of advanced-stage disease irrespective of the tumor anatomy. Templates of the treatment planning parameters will be developed for subgroups of these cases to improve the throughput in IMRT planning further. It is also expected that with better optimization algorithms, one could develop biologically based objective functions to optimize the intensity pattern, providing additional benefits.

Although IMRT may be effective in reducing normal tissue toxicity and improving tumor coverage, its high-dose gradient and conformity require a high level of precision in dose delivery and tumor localization. With the advent of functional imaging, such as positron emission tomography and other modalities, we may be able to address the challenges in tumor delineation more effectively. In the meantime, the complexity introduced by tumor motion must be recognized when using IMRT. Our current results are limited to the treatment planning study without fully accounting for the tumor motion and its impact on the accuracy of the IMRT dosimetry. For IMRT to be feasible and more effective in treating the NSCLC, motion reduction techniques should be explored further, such as those relying on respiratory gating, breath-hold, and tumor tracking. Although limited dosimetric evidence (27, 28) have shown that IMRT delivered through many fractions of the treatment may incur a similar magnitude of the dose spreading to a moving tumor compared with conventional 3D techniques, we believe that the safest way to deliver IMRT would still need to rely on effective motion control techniques. These techniques are currently under vigorous investigation at our clinic and will be the focus of our subsequent research.

## CONCLUSION

In this study, we compared IMRT and 3D-CRT plans in 41 NSCLC patients. The results showed that IMRT planning improved target conformity without significantly sacrificing the homogeneity of the tumor dose. The  $V_{10}$  and  $V_{20}$  of the normal lung decreased by a median of 7% and 10%, respectively, with IMRT. This resulted in a reduction in the mean lung dose of about 2 Gy and NTCP. In addition, IMRT reduced the irradiated volume of other critical structures, including the esophagus and heart. However, the  $V_5$  of thoracic tissue increased with IMRT. This increase was primarily caused by leakage of the MLC, which suggested the importance of additional improvement of the efficiency of the beam delivery IMRT system. IMRT may be a viable option for NSCLC with the possibility of minimizing normal tissue toxicity and/or dose escalation. The safety and feasibility of using IMRT for NSCLC must be further evaluated rigorously in carefully designed prospective clinical studies.

## REFERENCES

1. Parkin DM. Global cancer statistics in the year 2000. *Lancet Oncol* 2001;2:533–543.
2. Jemal A, Murray T, Samuels A, *et al*. Cancer statistics, 2003. *CA Cancer J Clin* 2003;53:5–26.
3. Arriagada R, Le Chevalier T, Quoix E, *et al*, for the GETCO, FNCLCC and the CEBI Trialists. ASTRO plenary: Effect of chemotherapy on locally advanced non-small cell lung carcinoma: A randomized study of 353 patients. *Int J Radiat Oncol Biol Phys* 1991;20:1183–1190.
4. Perez CA, Bauer M, Edelstein S, *et al*. Impact of tumor control

- on survival in carcinoma of the lung treated with irradiation. *Int J Radiat Oncol Biol Phys* 1986;12:539–547.
5. Vijayakumar S, Myriantopoulos LC, Rosenberg I, *et al.* Optimization of radical radiotherapy with beam's eye view techniques for non-small cell lung cancer. *Int J Radiat Oncol Biol Phys* 1991;21:779–788.
  6. Graham MV, Purdy JA, Emami B, *et al.* Clinical dose-volume histogram analysis for pneumonitis after 3D treatment for non-small cell lung cancer. *Int J Radiat Oncol Biol Phys* 1999;45:223–229.
  7. Sibley GS, Mundt AJ, Shapiro C, *et al.* The treatment of stage III non-small cell lung cancer using high dose conformal radiotherapy. *Int J Radiat Oncol Biol Phys* 1995;33:1001–1007.
  8. Armstrong J, Raben A, Zelefsky M, *et al.* Promising survival with three-dimensional conformal radiation for non-small cell lung cancer. *Radiother Oncol* 1997;44:17–22.
  9. Socinski MA, Rosenman JG, Halle J, *et al.* Dose-escalating conformal thoracic radiation therapy with induction and concurrent carboplatin/paclitaxel in unresectable stage IIIA/B non-small cell carcinoma: A modified phase I/II trial. *Cancer* 2001;92:1213–1223.
  10. Intensity-Modulated Radiation Therapy Collaborative Working Group. Intensity-modulated radiotherapy: Current status and issues of interest. *Int J Radiat Oncol Biol Phys* 2001;51:880–914.
  11. Van Sornsen de Kosta J, Voet P, Dirckx M, *et al.* An evaluation of two techniques for beam intensity modulation in patients irradiated for stage III non-small cell lung cancer. *Lung Cancer* 2001;32:145–153.
  12. Liu HH, Wang X, Dong L, *et al.* Feasibility of sparing the lung and other thoracic structures with intensity-modulated radiation therapy (IMRT) for non-small cell lung cancer. *Int J Radiat Oncol Biol Phys* 2004;58:1268–1279.
  13. Seppenwoolde Y, Shirato H, Kitamura K, *et al.* Precise and real-time measurement of 3D tumor motion in lung due to breathing and heartbeat, measured during radiotherapy. *Int J Radiat Oncol Biol Phys* 2002;53:822–834.
  14. Spirou SV, Chui CS. Generation of arbitrary intensity profiles by dynamic jaws or multileaf collimators. *Med Phys* 1994;21:1031–1041.
  15. Kutcher GJ, Burman C. Calculation of complication probability factors for non-uniform normal tissue irradiation: The effective volume method. *Int J Radiat Oncol Biol Phys* 1989;16:1623–1630.
  16. Lyman JT. Complication probability as assessed from dose volume histograms. *Radiat Res* 1985;104:S13–S19.
  17. Burman C, Kutcher GJ, Emami B, *et al.* Fitting of normal tissue tolerance data to an analytic function. *Int J Radiat Oncol Biol Phys* 1991;21:123–135.
  18. Emami B, Lyman J, Brown A, *et al.* Tolerances of normal tissue to therapeutic irradiation. *Int J Radiat Oncol Biol Phys* 1991;21:109–122.
  19. Hayman JA, Martel MK, Ten Haken RK, *et al.* Dose escalation in non-small-cell lung cancer using three dimensional conformal radiation therapy: Updated of a phase I trial. *J Clin Oncol* 2001;19:127–136.
  20. Graham MV, Purdy JA, Emami B, *et al.* Clinical dose-volume histogram analysis for pneumonitis after 3D treatment for non-small cell lung cancer (NSCLC). *Int J Radiat Oncol Biol Phys* 1999;45:323–329.
  21. Yorke ED, Jackson A, Rosenzweig KE, *et al.* Dose-volume factors contributing to the incidence of radiation pneumonitis in non-small-cell lung cancer patients treated with three-dimensional conformal radiation therapy. *Int J Radiat Oncol Biol Phys* 2002;54:329–339.
  22. Kwa SL, Lebesque JV, Theuvs JC, *et al.* Radiation pneumonitis as a function of mean lung dose: An analysis of pooled data of 540 patients. *Int J Radiat Oncol Biol Phys* 1998;42:1–9.
  23. Mohan R, Wu Q, Manning M, *et al.* Radiobiological considerations in the design of fractionation strategies for intensity-modulated radiation therapy of head and neck cancers. *Int J Radiat Oncol Biol Phys* 2000;46:619–630.
  24. Eisbruch A, Ship JA, Martel MK, *et al.* Parotid gland sparing in patients undergoing bilateral head and neck irradiation: Techniques and early results. *Int J Radiat Oncol Biol Phys* 1996;36:469–480.
  25. Xia P, Fu KK, Wong GW, *et al.* Comparison of treatment plans involving intensity-modulated radiotherapy for nasopharyngeal carcinoma. *Int J Radiat Oncol Biol Phys* 2000;48:329–337.
  26. Zelefsky MJ, Fuks Z, Hunt M, *et al.* High-dose intensity modulated radiation therapy for prostate cancer: Early toxicity and biochemical outcome in 772 patients. *Int J Radiat Oncol Biol Phys* 2002;53:1111–1116.
  27. Bortfeld T, Jokivarsi K, Goitein M, *et al.* Effects of intra-fraction motion on IMRT dose delivery: statistical analysis and simulation. *Phys Med Biol* 2002;47:2203–2220.
  28. Chui CS, Yorke E, Hong L. The effects of intra-fraction organ motion on the delivery of intensity-modulated field with a multileaf collimator. *Med Phys* 2003;30:1736–1746.